lele, Vang is recruited to the boundary between wild-type and mutant cells, whereas substantially less Vang is recruited to those boundaries in cells adjoining clones of the nonautonomous fz^{R52} allele (Fig. 4C, arrowheads). Thus, $Fz^{autonomous}$ proteins recruit Vang to the opposing cell surface, whereas nonautonomous alleles do not. The second prediction is that autonomous Fz proteins should fail to recruit Dsh. Indeed, we find that both are substantially impaired in Dsh recruitment, though somewhat less impaired than the very strong, nonautonomous fz^{R52} allele (Fig. 4D). Thus, strong *fz* alleles, many of which fail to accumulate Fz protein (*27*), display no or severely impaired interaction with Dsh and Vang, whereas autonomous alleles have impaired interaction with Dsh, but retain substantial ability to recruit Vang to the adjacent membrane. Notably, simulated overexpression of Fz with impaired Dsh interaction also produced the correct polarity disruption in cells proximal to the clones [fig. 9; (*17*)].

The Dsh^1 protein produces nearly autonomous clones, and it carries a mutation in its DEP domain, which is required for membrane localization (*16*, *19*); autonomous *fz* alleles bear point mutations in the first cytoplasmic loop (*27*), suggesting these mutations may affect the same interaction. A low affinity interaction between the Dsh PDZ domain and a sequence in the cytoplasmic tail of Fz has been demonstrated (*31*). Our data suggest that sequences in the Dsh DEP domain, and in the Fz first intracellular loop, are also important for Dsh membrane association. Thus, a regulated, bipartite, high affinity association of Dsh with Fz may be selectively disrupted in $fz^{autonomous}$ alleles.

The ability of our mathematical model to simultaneously reproduce all of the most characteristic PCP phenotypes (table S2) demonstrates the feasibility of the underlying biological model as a PCP signaling mechanism. Further, the mathematical model demonstrates how the overall scheme of the model—a local feedback loop between adjacent cells amplifying an initial asymmetry—can explain the autonomous and nonautonomous behavior of PCP mutant clones. Alternative models invoking diffusible factors have not been supported by the identification of such factors (*12*), and the contact-dependent intercellular signaling model more readily accounts for the slight nonautonomy of *dsh* and $fz^{autonomous}$ clones than do the diffusible factor models.

The ability of the mathematical model to make predictions and provide a detailed picture of PCP signaling is limited by the lack of complete biological understanding. Although the validity of quantitative model predictions is subject to its assumptions and the set of features used in parameter identification (SOM text), the model has allowed us to directly connect a biological model to the complex behaviors it was hypothesized to explain and to explore the implications of variations in the model.

References and Notes

1. P. N. Adler, *Dev. Cell* **2**, 525 (2002).
2. D. R. P. Tree, D. Ma, J. D. Axelrod, *Semin. Cell Dev. Biol.* **13**, 217 (2002).
3. J. Taylor, N. Abramova, J. Charlton, P. N. Adler, *Genetics* **150**, 199 (1998).
4. T. Wolff, G. M. Rubin, *Development* **125**, 1149 (1998).
5. D. Gubb, A. Garcia-Bellido, *J. Embryol. Exp. Morphol.* **68**, 37 (1982).
6. C. R. Vinson, P. N. Adler, *Nature* **329**, 549 (1987).
7. G. Struhl, D. A. Barbash, P. A. Lawrence, *Development* **124**, 2155 (1997).
8. M. Wehrli, A. Tomlinson, *Development* **125**, 1421 (1998).
9. P. A. Lawrence, J. Casal, G. Struhl, *Development* **126**, 2441 (1999).
10. P. N. Adler, J. Taylor, J. Charlton, *Mech. Dev.* **96**, 197 (2000).
11. D. Strutt, R. Johnson, K. Cooper, S. Bray, *Curr. Biol.* **12**, 813 (2002).
12. P. A. Lawrence, J. Casal, G. Struhl, *Development* **129**, 2749 (2002).
13. M. Fanto *et al.*, *Development* **130**, 763 (2003).
14. M. P. Zeidler, N. Perrimon, D. I. Strutt, *Genes Dev.* **13**, 1342 (1999).
15. P. A. Lawrence, J. Casal, G. Struhl, *Development* **131**, 4651 (2004).
16. J. D. Axelrod, *Genes Dev.* **15**, 1182 (2001).
17. D. I. Strutt, *Mol. Cell* **7**, 367 (2001).
18. D. R. P. Tree *et al.*, *Cell* **109**, 371 (2002).
19. J. D. Axelrod, J. R. Miller, J. M. Shulman, R. T. Moon, N. Perrimon, *Genes Dev.* **12**, 2610 (1998).
20. D. Gubb *et al.*, *Genes Dev.* **13**, 2315 (1999).
21. R. Bastock, H. Strutt, D. Strutt, *Development* **130**, 3007 (2003).
22. C. Yang, J. D. Axelrod, M. A. Simon, *Cell* **108**, 675 (2002).
23. D. Ma, C. H. Yang, H. McNeill, M. A. Simon, J. D. Axelrod, *Nature* **421**, 543 (2003).
24. J. Casal, G. Struhl, P. Lawrence, *Curr. Biol.* **12**, 1189 (2002).
25. M. Hannus, F. Feiguin, C. P. Heisenberg, S. Eaton, *Development* **129**, 3493 (2002).
26. H. Strutt, D. Strutt, *Dev. Cell* **3**, 851 (2002).
27. K. H. Jones, J. Liu, P. N. Adler, *Genetics* **142**, 205 (1996).
28. A. M. Turing, *Philos. Trans. R. Soc. London B Biol. Sci.* **237**, 37 (1952).
29. P. N. Adler, personal communication.
30. K. Amonlirdviman, unpublished observations.
31. H. C. Wong *et al.*, *Mol. Cell* **12**, 1251 (2003).

32. This work was supported by the Defense Advanced Research Projects Agency BioInfoMicro (C.J.T.) and BioComp (C.J.T. and J.D.A.) Programs, Stanford's Bio-X IIP (J.D.A. and C.J.T.), NIH R01-GM59823 (J.D.A.), a National Defense Science and Engineering Graduate fellowship (K.A.), a Burt and Deedee McMurtry Stanford Graduate Fellowship (K.A.) and a PHS grant awarded by the National Cancer Institute, DHHS (W.-S.C.). We thank H. McAdams for the initial suggestion of the problem and R. Ghosh for contributions to the mathematical model.

Supporting Online Material

www.sciencemag.org/cgi/content/full/307/5708/423/DC1
Materials and Methods
SOM Text
Figs. S1 to S16
Tables S1 and S2
References and Notes

21 September 2004; accepted 29 November 2004
10.1126/science.1105471

Visfatin: A Protein Secreted by Visceral Fat That Mimics the Effects of Insulin

Atsunori Fukuhara,[1,2*] Morihiro Matsuda,[1*] Masako Nishizawa,[3*] Katsumori Segawa,[1] Masaki Tanaka,[1] Kae Kishimoto,[3] Yasushi Matsuki,[3] Mirei Murakami,[4] Tomoko Ichisaka,[4] Hiroko Murakami,[3] Eijiro Watanabe,[3] Toshiyuki Takagi,[1] Megumi Akiyoshi,[3] Tsuguteru Ohtsubo,[3] Shinji Kihara,[5] Shizuya Yamashita,[5] Makoto Makishima,[1] Tohru Funahashi,[5] Shinya Yamanaka,[4] Ryuji Hiramatsu,[3] Yuji Matsuzawa,[6] Iichiro Shimomura[1,5,7]†

Fat tissue produces a variety of secreted proteins (adipocytokines) with important roles in metabolism. We isolated a newly identified adipocytokine, visfatin, that is highly enriched in the visceral fat of both humans and mice and whose expression level in plasma increases during the development of obesity. Visfatin corresponds to a protein identified previously as pre–B cell colony-enhancing factor (PBEF), a 52-kilodalton cytokine expressed in lymphocytes. Visfatin exerted insulin-mimetic effects in cultured cells and lowered plasma glucose levels in mice. Mice heterozygous for a targeted mutation in the visfatin gene had modestly higher levels of plasma glucose relative to wild-type littermates. Surprisingly, visfatin binds to and activates the insulin receptor. Further study of visfatin's physiological role may lead to new insights into glucose homeostasis and/or new therapies for metabolic disorders such as diabetes.

Recent work in obesity research has revealed that adipose tissue functions as an endocrine organ, producing a variety of secreted factors including leptin (*1*), adiponectin/ACRP30/AdipoQ (*2*–*4*), tumor necrosis factor–α (TNF-α) (*5*), resistin (*6*), and plasminogen

activator inhibitor–1 (*7*). These so-called adipocytokines play important roles in metabolic homeostasis, and when their production is not properly regulated, they can contribute to metabolic diseases and atherosclerosis (*8*, *9*).

We sought to identify new adipocytokine(s) that are preferentially produced by human abdominal visceral fat, the accumulation of which has been linked to metabolic syndrome (*10*–*12*). Using a differential display method, we compared 8800 polymerase chain reaction (PCR) products from cDNAs derived from paired samples of subcutaneous fat and visceral fat, obtained from two female volunteers. A total of 31 bands were detected exclusively in the visceral fat samples (Fig. 1A). When used as a probe on Northern blots, one of these cDNAs detected mRNA that was more abundantly expressed in visceral fat than in subcutaneous fat (Fig. 1B). Sequencing revealed that this cDNA fragment corresponds to the 5′-untranslated region of the gene encoding pre-B cell colony-enhancing factor (PBEF) (GenBank accession number U02020) (*13*). PBEF is a growth factor for early-stage B cells and is a secreted protein mainly expressed in bone marrow, liver, and muscle (*13*). Recently, Marshall and colleagues reported that PBEF inhibits neutrophil apoptosis in clinical and experimental sepsis (*14*). A rabbit polyclonal antibody to human PBEF detected a 52-kD protein in the medium as well as the lysate of COS-1 cells transfected with the gene encoding PBEF. The same antibody detected a protein of similar size in human and mouse plasma (Fig. 1C). During differentiation of 3T3-L1 adipocytes in vitro, PBEF mRNA expression increased markedly (Fig. 1D, top), and this was accompanied by secretion of PBEF protein into the medium (Fig. 1D, bottom).

To investigate the relationship between serum levels of PBEF and adiposity, we studied both humans and mice. In 101 male and female human subjects, plasma PBEF concentrations correlated strongly with the amount of visceral fat as estimated by computed tomography ($r = 0.68$, $P < 0.001$) but only weakly with the amount of subcutaneous fat ($r = 0.22$, $P < 0.05$) (Fig. 1E). We also analyzed KKAy mice, a model for obese type II diabetes. KKAy mice rapidly become obese between 6 and 12 weeks of age (Fig. 1F). We found that during this time period, plasma PBEF levels increased significantly (Fig. 1G), as did PBEF mRNA levels in visceral fat (Fig. 1H). In contrast, PBEF mRNA levels in subcutaneous fat and liver changed very little. Finally, we measured plasma PBEF levels in c57BL/6J mice fed a normal chow diet or a high-fat/high-sucrose diet. Mice on the high-fat diet had higher plasma PBEF concentrations relative to mice fed normal chow (9.94 ± 1.70 pM versus 6.86 ± 1.35 pM, mean ± SD; $P < 0.05$), and this was accompanied by a significant increase in PBEF mRNA levels in visceral mesenteric fat (*15*). These results suggest that PBEF is a secreted factor produced abundantly by visceral fat; we therefore refer to it as visfatin.

Assessment of the biological function of visfatin revealed that it has a glucose-lowering effect. Acute administration of recombinant visfatin to c57BL/6J mice by intravenous injection resulted in a statistically significant fall in plasma glucose levels within 30 min (Fig. 2A). This effect was dose-dependent and was not due to changes in plasma insulin levels (Fig. 2B). We next injected visfatin into insulin-resistant obese KKAy mice. Visfatin significantly reduced plasma glucose concentrations, and the effect was similar to that induced by insulin injection (Fig. 2C). Similar results were seen with streptozotocin (STZ)–treated insulin-deficient mice (Fig. 2D). To investigate the effects of chronic administration of visfatin, we infected c57BL/6J and KKAy mice with an adenovirus vector encoding visfatin or LacZ (Fig. 2, E and F). Plasma visfatin

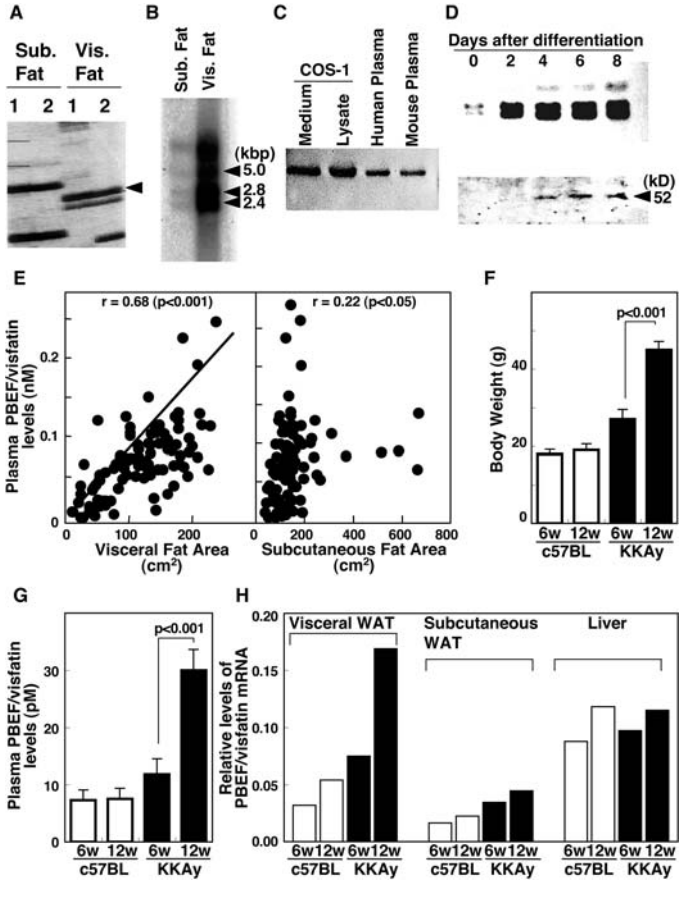

Fig. 1. Identification, expression, and secretion of PBEF/visfatin. (**A**) Differential display using paired samples of human visceral and subcutaneous fat from two female volunteers. Arrowhead indicates PCR fragment equivalent to PBEF/visfatin. (**B**) Northern blotting of PBEF/visfatin mRNA in human visceral and subcutaneous fat, using the cDNA fragment in (A) as a probe. (**C**) Immunoblotting of PBEF/visfatin protein in cell culture medium, cell lysate, and plasma from humans and mice. COS-1 cells were transfected with PBEF/visfatin expression vector. (**D**) Northern blotting of PBEF/visfatin mRNA in vitro (top) and immunoblotting of PBEF/visfatin protein secreted into the culture medium during this process (bottom). (**E**) Correlation between plasma PBEF/visfatin levels and visceral fat area (left) or subcutaneous fat area (right) in 101 male and female human subjects. (**F**) Body weight of male c57BL/6J and KKAy mice at 6 and 12 weeks of age (six mice per group). (**G**) Plasma PBEF/visfatin levels in male c57BL/6J and KKAy mice at 6 and 12 weeks of age (six mice per group). (**H**) Relative abundance of PBEF/visfatin mRNA in visceral fat, subcutaneous fat, and liver of 6- and 12-week-old male c57BL/6J and KKAy mice. Pooled total RNA from six mice per group was subjected to real-time reverse transcription PCR. The expression level of PBEF/visfatin mRNA was compared with that of cyclophilin mRNA. WAT, white adipose tissue. All data are expressed as means ± SD. Differences between groups were examined for statistical significance with Student's *t* test.

[1]Department of Medicine and Pathophysiology, Graduate School of Medicine, and Department of Organismal Biosystems, Graduate School of Frontier Biosciences, Osaka University, 2-2 Yamadaoka, Suita, Osaka 565-0871, Japan. [2]Japan Society for the Promotion of Science, Ichibancho, Chiyoda-ku, Tokyo 102-8471, Japan. [3]Genomic Science Laboratories, Sumitomo Pharmaceuticals Co. Ltd., 2-1, Takatsukasa 4-Chome, Takarazuka, Hyogo 665-0051, Japan. [4]CREST, JST, Laboratory of Animal Molecular Technology, Research and Education Center for Genetic Information, Nara Institute of Science and Technology, Ikoma, Nara 630-0192, Japan. [5]Department of Internal Medicine and Molecular Science, Graduate School of Medicine, Osaka University, 2-2 Yamadaoka, Suita, Osaka 565-0871, Japan. [6]Sumitomo Hospital, 5-3-20 Nakanoshima, Kita-Ku, Osaka, 530-0005, Japan. [7]PRESTO, Japan Science and Technology Agency, 4-1-8 Honcho, Kawaguchi, Saitama 332-0012, Japan.

*These authors contributed equally to this work.
†To whom correspondence should be addressed. E-mail: ichi@imed2.med.osaka-u.ac.jp

levels almost doubled upon adenoviral infection (*15*). Chronic production of visfatin via the adenovirus significantly attenuated plasma glucose and insulin levels in both strains of mice (Fig. 2, E and F).

To explore the physiological function of visfatin, we generated visfatin-deficient (visfatin$^{-/-}$) mice. The visfatin$^{-/-}$ mice died during early embryogenesis, so we analyzed heterozygous (visfatin$^{+/-}$) mice. These mice were viable, and their plasma visfatin levels were about two-thirds those of wild-type mice (wild type, 7.2 ± 0.5 pM; visfatin$^{+/-}$, 4.8 ± 0.3 pM). There were no differences in growth rate, food intake, total body weight, and tissue weight of epididymal fat, brown fat, liver, gastrocnemius muscle, and heart between wild-type and visfatin$^{+/-}$ mice. Plasma insulin levels did not differ significantly between these mice (wild type, 0.9 ± 0.2 ng/ml; visfatin$^{+/-}$, 1.0 ± 0.3 ng/ml). However, plasma glucose levels were higher in the visfatin$^{+/-}$ mice under both fasting and feeding conditions. This effect was modest but statistically significant (Fig. 2G). Glucose tolerance tests showed that the plasma glucose levels of visfatin$^{+/-}$ mice were modestly higher than those of wild-type mice at 60 and 120 min after glucose overload (Fig. 2H). Insulin tolerance tests showed similar insulin sensitivity in visfatin$^{+/-}$ and wild-type mice (*15*). These analyses indicate that, like insulin, visfatin has a physiological role in lowering plasma glucose levels.

To examine the insulin-mimetic effects of visfatin in more detail, we studied a variety of cultured cells. Visfatin treatment enhanced glucose uptake in 3T3-L1 adipocytes (Fig. 3A) and L6 myocytes (Fig. 3B) and suppressed glucose release in H4IIEC3 hepatocytes (Fig. 3C). These effects were similar to those of insulin (Fig. 3, A to C). We also examined the effect of visfatin on adipocyte differentiation. Primary-cultured preadipocytes from visceral mesenteric (Fig. 3D, left) and subcutaneous (Fig. 3D, right) fat depots of control ICR (Institute for Cancer Research) mice were treated with phosphate-buffered saline (PBS), visfatin, or insulin. Like insulin, visfatin induced triglyceride accumulation in preadipocytes from both fat depots and accelerated triglyceride synthesis from glucose (Fig. 3E) (fig. S1). Visfatin treatment also markedly induced the expression of genes encoding adipose markers such as peroxisome proliferator-activated receptor–γ (PPAR-γ), CCAAT-enhancer binding protein–α (C/EBP-α), fatty acid synthase (FAS), diacylglycerol *O*-acyltransferase–1 (DGAT-1), adipose P2 (aP2), and adiponectin (fig. S2). Similar adipogenesis-inducing effects of visfatin were observed in 3T3-L1 and 3T3-F442A cells (*15*).

We next investigated whether visfatin had an effect on insulin signaling. Intravenous injection of visfatin into mice induced tyrosine phosphorylation of the insulin receptor (IR), insulin receptor substrate–1 (IRS-1), and IRS-2 in the liver, similar to the effects of insulin injection (Fig. 4A). Visfatin treatment of 3T3-F442A adipocytes in culture induced the phosphorylation of IR, IRS-1, and IRS-2; binding of phosphatidylinositol 3-kinase (PI3K) to IRS-1 and IRS-2; and phosphorylation of Akt and mitogen-activated protein kinase (MAPK), again resembling the effects of insulin (Fig. 4B). Similar activation of the insulin signal transduction pathway was observed in L6 myocytes (Fig. 4C) and H4IIEC3 hepatocytes (Fig. 4D). Visfatin also enhanced IRS-1–associated PI3K activity in epididymal fat–derived primary adipocytes, and the effect of visfatin and insulin was additive in this assay (Fig. 4E).

We also analyzed the binding affinity of visfatin to IR. Expression of IR at the cell surface in human embryonic kidney (HEK) 293 cells enhanced the binding of both visfatin and insulin to cells (Fig. 4F). The binding equilibrium dissociation constant (K_D) of visfatin to IR (4.4 nM) was similar to that of insulin (6.1 nM). However, binding of visfatin to insulin-like growth factor I receptor (IGF-IR) was very weak (fig. S3). We also found that visfatin binds to immunoprecipitated IR protein from HEK-293 cells transfected with the gene encoding IR (Fig. 4G).

To determine whether insulin and visfatin share a common binding site in IR, we used a competitive inhibition assay. Unlabeled insulin displaced radiolabeled insulin binding to IR expressed in intact HEK-293 cells, but unlabeled visfatin did not (Fig. 4H, top). Similarly, unlabeled visfatin displaced radiolabeled visfatin binding to IR, but unlabeled insulin did not (Fig. 4H, bottom). We also investigated whether visfatin bound to IR with an Asn^{15} → Lys mutation in the α-subunit (IR-N15K). Insulin binds to the extracellular α-subunit of IR, and N15K mutant was reported to cause loss of binding affinity of insulin (*16*). As previously described, the binding affinity of IR-N15K to insulin (K_D = 69.7 nM) was blunted relative to that of wild-type IR (IR-

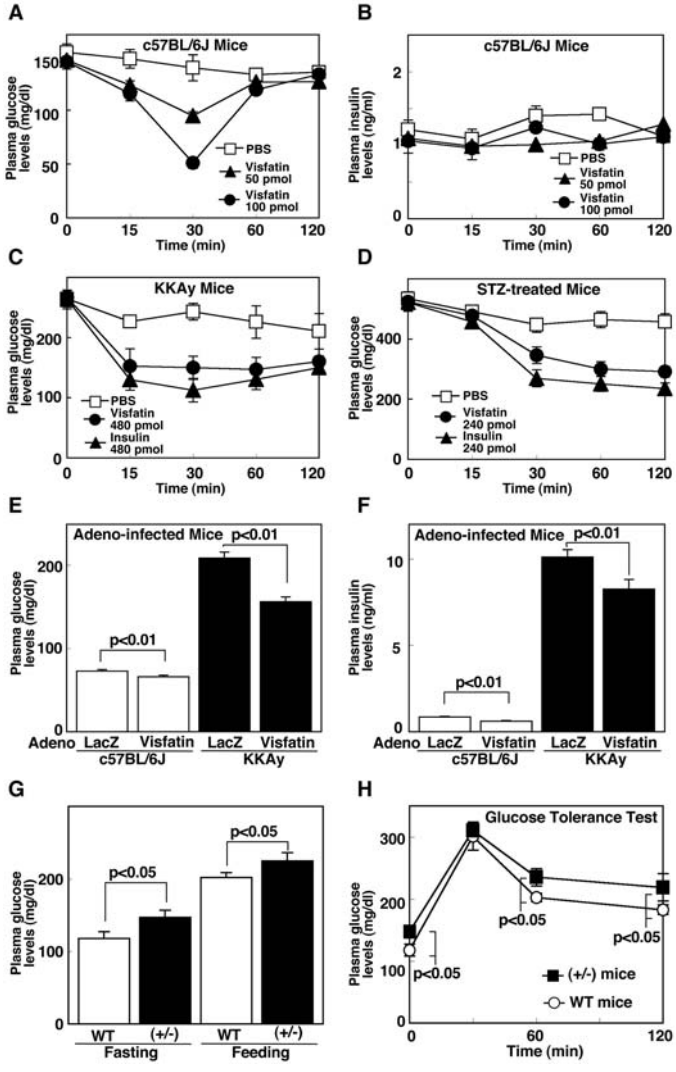

Fig. 2. Glucose-lowering effects of visfatin in mouse models. (**A** and **B**) Plasma glucose (A) and insulin (B) concentrations in male c57BL/6J mice after a single-bolus injection of PBS or visfatin (five mice per group). (**C** and **D**) Plasma glucose concentrations in male KKAy mice (C) and STZ-treated male c57BL/6J mice (D) after a single-bolus injection of PBS, visfatin, or insulin (five mice per group). (**E** and **F**) Fasting plasma glucose (E) and insulin levels (F) in male c57BL/6J and KKAy mice at day 7 after infection with an adenovirus vector expressing the LacZ gene product or visfatin (10 mice per group). (**G**) Plasma glucose levels in male wild-type and visfatin$^{+/-}$ mice in 12-hour fasting or feeding conditions (seven mice per group). (**H**) Glucose tolerance test in male wild-type and visfatin$^{+/-}$ mice (seven mice per group). All data are expressed as means ± SD. Differences between groups were examined for statistical significance with Student's *t* test.

WT) to insulin (K_D = 2.5 nM) (Fig. 4I, top). However, visfatin potently bound to IR-N15K (K_D = 6.6 nM), comparable to the binding of visfatin to IR-WT (K_D = 3.0 nM) (Fig. 4I, bottom). Indeed, we also observed visfatin-dependent autophosphorylation of IR-N15K in intact CHO cells expressing IR-N15K (*15*). These results suggest that visfatin directly activates IR but in a manner distinct from insulin.

In summary, several lines of evidence indicate that visfatin shares properties with insulin both in vivo and in vitro. First, administration of high doses of recombinant visfatin lowered plasma glucose levels in both

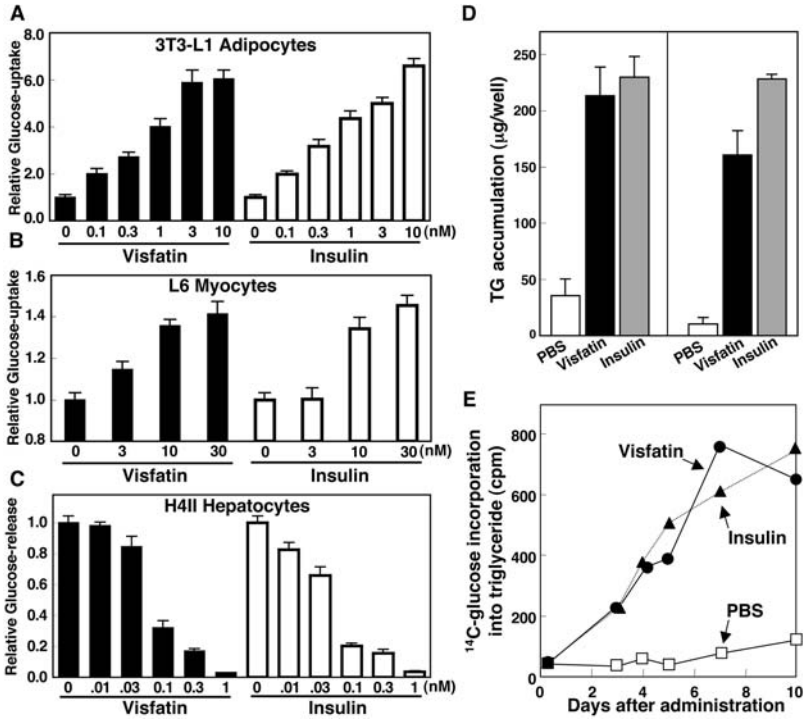

Fig. 3. Effects of visfatin in cultured cells. (**A** to **C**) Effects of visfatin and insulin on glucose uptake in 3T3-L1 adipocytes (A) and L6 myocytes (B) and on glucose release into medium in H4IIEC3 hepatocytes (C). Data are expressed as means ± SD of three experiments performed in duplicate. (**D** and **E**) Effects of visfatin and insulin on triglyceride accumulation. Preadipocytes obtained from visceral mesenteric [(D), left] or subcutaneous [(D), right] fat depots of control male ICR mice were cultured with visfatin or insulin (10 ng/ml each) for 6 days. Accumulated triglyceride (TG) was measured. (E) ^{14}C-glucose incorporation into triglycerides. All data shown are means ± SD.

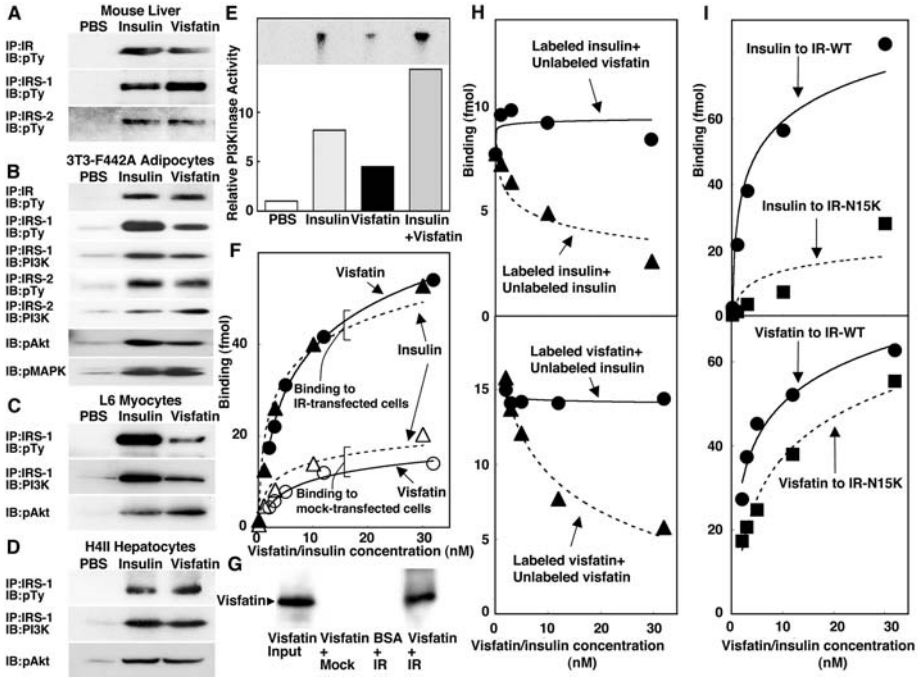

Fig. 4. Effects of visfatin on insulin signal transduction. (**A**) Tyrosine phosphorylation of IR, IRS-1, and IRS-2 in mouse liver after delivery of 240 pmol of insulin or visfatin by injection into the jugular vein. The liver was removed 10 min after injection, and the protein extract was analyzed by immunoprecipitation (IP) with antibodies to IR, IRS-1, and IRS-2 after immunoblotting (IB) with antibody to phosphotyrosine (pTy). (**B**) Tyrosine phosphorylation of IR, IRS-1, and IRS-2 and serine phosphorylation of Akt and MAPK in cultured 3T3-F442A adipocytes after treatment with PBS, insulin (100 ng/ml), or visfatin (100 ng/ml). (**C** and **D**) Tyrosine phosphorylation of IRS-1, serine phosphorylation of Akt, and amounts of PI3K bound to IRS-1 in L6 myocytes (C) or H4IIEC3 hepatocytes (D). Cells were treated with PBS, insulin (100 ng/ml), or visfatin (100 ng/ml). For measurement of serine phosphorylation of Akt and MAPK, proteins were separated by electrophoresis, blotted onto a membrane, and detected with antibodies to phospho-Akt and phospho-MAPK. For measurement of IRS-1 and IRS-2, the protein extracts were analyzed by immunoprecipitation with antibodies to IRS-1 and IRS-2 and detected with antibodies to phosphotyrosine and PI3K. (**E**) IRS-1–associated PI3K activity in primary adipocytes from epididymal fat depots of c57BL/6J mice treated as in (B). (Inset) ^{32}P-labeled 3-phosphatidylinositides. (**F**) Binding of ^{125}I-labeled insulin (triangles) or visfatin (circles) to intact HEK-293 cells transfected with plasmid alone or plasmid encoding IR. (**G**) Direct binding of visfatin to human IR in vitro. Purified visfatin or bovine serum albumin (BSA) was incubated with Flag-IR or Flag alone immobilized on anti-Flag beads. The beads were extensively washed and subjected to SDS–polyacrylamide gel electrophoresis followed by Western blotting with antibody to visfatin. (**H**) (Top) Competitive inhibition of binding of ^{125}I-labeled insulin by unlabeled visfatin or insulin to intact HEK-293 cells transfected with IR. (Bottom) Competitive inhibition of binding of ^{125}I-labeled visfatin by unlabeled insulin or visfatin to intact HEK-293 cells transfected with IR. (**I**) Binding of ^{125}I-labeled insulin (top) or visfatin (bottom) to intact HEK-293 cells transfected with IR-WT or IR-N15K vector.

insulin-resistant and insulin-deficient mice. Second, in obese KKAy mice, a doubling of plasma visfatin levels achieved by an adenovirus vector also led to a reduction of plasma glucose and insulin concentrations. Finally, our biochemical studies indicate that visfatin activates insulin signaling through IR but in a different fashion from insulin.

There are important differences between visfatin and insulin, however. Plasma visfatin levels did not change significantly upon fasting or feeding in mice (fig. S4), whereas plasma insulin levels increased in the fed state and decreased in the fasting state. The plasma concentration of visfatin was 10% that of insulin in the fasting condition and only 3% in the fed condition. These low concentrations of visfatin may account for the modest effect of visfatin on plasma glucose levels relative to that of insulin, as shown by our analysis of visfatin$^{+/-}$ mice. Our biochemical studies showed that at similar concentrations, visfatin and insulin have a comparable ability to activate insulin signaling and glucose uptake and to inhibit glucose release. Moreover, in visfatin$^{+/-}$ mice, a 3 pM reduction in plasma visfatin levels leads to a 10 to 20 mg/dl elevation in plasma glucose concentrations. Taken together, these data suggest that visfatin plays a physiological role in lowering plasma glucose concentrations, but its contribution is small because of its low concentration.

The previously reported function of PBEF/visfatin was enhancement of the effect of interleukin-7 (IL-7) on pre-B cell colony formation (*13*). Insulin and IGFs were also reported to potentiate pre-B cell colony formation (*17*). Thus, this function of PBEF/visfatin may be attributed to another insulin-like effect. Relative to adipose tissue of lean mice, adipose tissue of obese mice contains increased amounts of proinflammatory cytokines such as TNF-α or IL-6. Both of these cytokines increase mRNA levels of PBEF/visfatin (*18*) and thus may be responsible for the increased mRNA levels of PBEF/visfatin in visceral fat.

The discovery of the insulin-mimetic function of visfatin may shed new light on glucose and lipid homeostasis, adipocyte proliferation and differentiation, and other aspects of insulin-related biology. The potential relationship between visfatin and metabolic syndrome also merits further investigation, because plasma visfatin levels increase in proportion to visceral fat accumulation. Finally, our results raise the possibility that visfatin may be a useful target for the development of drug therapies for diabetes.

References and Notes

1. J. M. Friedman, J. L. Halaas, *Nature* **395**, 763 (1998).
2. K. Maeda *et al.*, *Biochem. Biophys. Res. Commun.* **221**, 286 (1996).
3. P. E. Scherer, S. Williams, M. Fogliano, G. Baldini, H. F. Lodish, *J. Biol. Chem.* **270**, 26746 (1995).
4. E. Hu, P. Liang, B. M. Spiegelman, *J. Biol. Chem.* **271**, 10697 (1996).
5. G. S. Hotamisligil, N. S. Shargill, B. M. Spiegelman, *Science* **259**, 87 (1993).
6. C. M. Steppan *et al.*, *Nature* **409**, 307 (2001).
7. I. Shimomura *et al.*, *Nature Med.* **2**, 800 (1996).
8. I. Shimomura, R. E. Hammer, S. Ikemoto, M. S. Brown, J. L. Goldstein, *Nature* **401**, 73 (1999).
9. N. Maeda *et al.*, *Nature Med.* **8**, 731 (2002).
10. A. H. Kissebah, A. N. Peiris, *Diabetes Metab. Rev.* **5**, 83 (1989).
11. Y. Matsuzawa, I. Shimomura, T. Nakamura, Y. Keno, K. Tokunaga, *Ann. N. Y. Acad. Sci.* **676**, 270 (1993).
12. S. Fujioka, Y. Matsuzawa, K. Tokunaga, S. Tarui, *Metabolism* **36**, 54 (1987).
13. B. Samal *et al.*, *Mol. Cell. Biol.* **14**, 1431 (1994).
14. S. H. Jia *et al.*, *J. Clin. Invest.* **113**, 1318 (2004).
15. A. Fukuhara *et al.*, unpublished data.
16. T. Kadowaki, H. Kadowaki, D. Accili, S. I. Taylor, *J. Biol. Chem.* **265**, 19143 (1990).
17. K. S. Landreth, R. Narayanan, K. Dorshkind, *Blood* **80**, 1207 (1992).
18. S. Ognjanovic *et al.*, *J. Mol. Endocrinol.* **26**, 107 (2001).

19. We thank the members of the Shimomura laboratory for helpful discussions, D. Accili and S. Takahashi for the IGF-IR expression vector, and H. Kondo for the visfatin-producing adenovirus. Supported by the 21st Century Center of Excellence Program; the Japan Research Foundation for Clinical Pharmacology; the Ministry of Health, Labor and Welfare, Japan; and the Ministry of Education, Culture, Sports, Science and Technology, Japan.

Supporting Online Material

www.sciencemag.org/cgi/content/full/1097243/DC1
Materials and Methods
Figs. S1 to S4

26 February 2004; accepted 29 October 2004
Published online 16 December 2004;
10.1126/science.1097243
Include this information when citing this paper.

T Helper Cell Fate Specified by Kinase-Mediated Interaction of T-bet with GATA-3

Eun Sook Hwang,[1] Susanne J. Szabo,[1]* Pamela L. Schwartzberg,[3] Laurie H. Glimcher[1,2]†

Cell lineage specification depends on both gene activation and gene silencing, and in the differentiation of T helper progenitors to Th1 or Th2 effector cells, this requires the action of two opposing transcription factors, T-bet and GATA-3. T-bet is essential for the development of Th1 cells, and GATA-3 performs an equivalent role in Th2 development. We report that T-bet represses Th2 lineage commitment through tyrosine kinase–mediated interaction between the two transcription factors that interferes with the binding of GATA-3 to its target DNA. These results provide a novel function for tyrosine phosphorylation of a transcription factor in specifying alternate fates of a common progenitor cell.

The immune system T-box protein T-bet controls lineage commitment of the two subsets of cytokine-producing helper T cells, Type 1 (Th1) and Type 2 (Th2) (*1*–*3*) by simultaneously driving Th1 genetic programs and repressing the development of the opposing Th2 subset. T-bet is principally required for expression of the potent inflammatory cytokine interferon-γ (IFN-γ), the hallmark of Type 1 immunity, and simultaneous repression of the signature Th2 cytokines interleukin-4 (IL-4) and IL-5 (*1*, *4*). As a consequence, mice lacking T-bet fail to develop a Th1 compartment but possess an overexpanded Th2 compartment, which leads to a spontaneous asthma-related phenotype (*2*, *5*). Although it is established that T-bet accomplishes Th1 programs partly through direct induction of IFN-γ– and IL-12Rβ2–chain gene transcription (*6*), the mechanism by which it represses Th2 programs is unclear.

To determine whether T cell receptor (TCR) signaling induced alterations in T-bet, a Th1 clone and control Th2 clone were tested after polyclonal TCR engagement. Western blotting revealed a specific phosphorylated species in a Th1 clone that was not present in Th2 cells (fig. S1A). T-bet was rapidly induced in early Th1 differentiation, gradually decreasing at later stages (Fig. 1A). We also observed T-bet tyrosine phosphorylation to occur primarily in Thp cells upon TCR engagement, being most pronounced early in differentiation (day 2), declining by day 4, and being undetectable upon secondary stimulation (Fig. 1A). Tyrosine phosphorylation of T-bet was also enhanced in the presence of the phosphatase inhibitor pervanadate (fig. S1B). Thus, T-bet becomes tyrosine phosphorylated at the earliest stages of Thp dif-

[1]Department of Immunology and Infectious Diseases, Harvard School of Public Health, and [2]Department of Medicine, Harvard Medical School, Boston, MA 02115, USA. [3]National Human Genome Research Institute, National Institutes of Health, Bethesda, MD 20892, USA.

*Present address: Novartis Pharmaceuticals, Cambridge, MA 02115, USA.

†To whom correspondence should be addressed. E-mail: lglimche@hsph.harvard.edu